Chemistry and Materials Research
ISSN 2224- 3224 (Print) ISSN 2225- 0956 (Online)
Vol.10 No.7, 2018

Electroless plating of Ni-B composite coating on AZ31 Mg alloy

Salah Eldin k. A. Abdulhamid[1], Ibrahim M Ghayad[2], Fatma Kandemirli[1],

[1] Department of Material Science, Kastamonu University, Turkey
[2] Central Metallurgical R& D Institute, Egypt
*E-mail: ighayad@yahoo.com

Abstract
A Ni–B coating was electroless-deposited directly on H_3PO_4/HF pickled AZ31. The thickness of the plating layer was estimated through weight gain measurements and was affected by temperature, time and bath composition. The highest thickness was obtained at 6 g/L of $NaHB_4$ at 85°C. An adherent compact layer of Ni-B was obtained. Electrochemical impedance spectroscopy measurements in 3.5 wt.% sodium chloride aqueous solution suggest that the plating can protect the magnesium alloy substrate from corrosion attack.

Introduction
Magnesium and its alloys are more and more applied in different sectors, including aircraft, motor vehicle as well as metallurgical, chemical and electrical industries. As a light metal having a density of 1.74 g/cm^3, it is 35% lighter than aluminum (2.7 g/cm^3) and over four times lighter than steel (7.86 g/cm^3). Today's interest in magnesium alloys for automotive applications is based on a combination of high strength properties and low density. Magnesium alloys are very attractive as structural materials mostly in applications where weight saving is of great concern. Mg-Al alloy is the most common category of magnesium alloys. Aluminum has a strong passivation tendency in presence of oxygen and results in the precipitation of β phase, which is highly cathodic with respect to the matrix [1,2].

Magnesium and its alloys has a poor corrosion resistance which can be attributed to the extremely electronegative potential of Mg making it exceptionally prone to galvanic corrosion when internal coupled with more noble potentials (e.g. impurities or second phases) or by external coupling with dissimilar metals. The oxide film formed on its surface is of poor quality and has relatively low resistance to corrosion. This "quasi-passivity" of Mg causes poor pitting resistance of both pure magnesium and its alloys. Oxide films formed on magnesium also tend to dissolve in water or breakdown chemically in many environments, namely; chloride, bromide, sulfate, nitrate, and chromate [3]. AZ31B is a wrought magnesium alloy with good room-temperature strength and ductility combined with corrosion resistance and weldability. AZ31B finds application in wide variety of uses including aircraft fuselages, cell phone and laptop cases, speaker cones and concrete tools. AZ31B can be super formed at elevated temperatures to produce a wide variety of intricate components for automotive uses [4].

The following section will through light on the published papers focused on the electroless Ni-B plating on Mg and its alloys. Shao et al [5] investigated the effect of three acid pickling and activation solutions on the electroless Ni-P plating on AZ91 Mg alloy. Results showed that pickling in $HNO_3$25ml/L, H_3PO_4 25 ml/Land activation in $NH_4H_2PO_4$80–100 g/L, NH_4F 30–50 g/L at room temperature, AZ91 could be directly electroless plated. The structure of Ni–P coating was uniform, amorphous highly resistant towards corrosion.Correa et al [6] have deposited Ni–B coatings directly on commercial purity magnesium and AZ91D magnesium alloy by a chromium-free electroless process. A cauliflower-type coatingwas obtained at a rate of ~8 to 13 μm/h. The addition of $NH_4HF_2$to the electroless bath improves the coatings corrosion resistance when tested in sodium chloride solution.Wang et al [7] briefly reviewed current electroless plating techniques for Mg alloys with especial attention to Ni-B plating. Ni-B plating methodology and its electroless plating mechanism was proposed. The deposited Ni-B layer on AZ91D is then systematically characterized for its microstructure, porosity, thickness, adhesion and corrosion resistance. Bülbül [8] has produced about 6 μm Ni-B coating on AZ91 Mg alloy using electroless plaring technique. The coating showed a high degree of surface roughness (from 0.8 μm to 1.95 μm). XRD analysis showed an amorphous Ni–B coating.Wang et al [9] deposited Ni–B coating directly on acetic acid pickled AZ91D. The electroless Ni–B plating exhibits a uniform surface and an amorphous structure with a high corrosion resistance. Correa et al [10] employed non-chromate-based electroless Ni-B coatings on pure magnesium and AZ91D alloy. No chemical activation of the substrate was done before plating. Etching of the substrates develops an oxide layer on the surface of both substrates. The oxide is thicker on the magnesium than on the alloy while an enrichment of zinc between the bulk substrate and the oxide layer occurs in the case of the AZ91D alloy. Ni-B coatings improved wear resistance of both substrates. Bonin et a l [11] investigated the Ni-B coatings fabricated by electroless deposition using either ultrasonic or mechanical agitation in an aqueous bath containing nickel chloride, sodium borohydride, ethylene diamine and lead tungstate at pH 12 ± 1. The results showed that low frequency ultrasonic agitation increases the coatings thickness by over 50% compared to those produced using mechanical agitation. Zhang et al [12] successfully fabricated electroless double-layered Ni-B/Ni-P coating on AZ91D Mg alloy by plating of a Ni-B layer as primer and a Ni-P layer as outer layer from eco-friendly fluoride-free plating baths. The new-designed duplex coating also exhibits a remarkable enhancement in micro-hardness.In the work of Correa et al [13], the wear rates of elecctroless Ni–B coatings on commercial purity magnesium and AZ91D alloy were two magnitude orders lower than substrates. The wear mechanism of the electroless Ni–B coatings was governed by the presence of abrasive wear, delamination and tribo-corrosion processes. Mukhopadhyay, et al [14] investigated the electroless deposition and tribological behavior of a ternary variant of the borohydride reduced coating i.e. Ni-B-Won AISI 1040 steel substrates. Heat treatment at 500°C transforms the amorphous morphology of the coating into crystalline one. Heat treatment improved the microhardness and enhanced the tribological behavior of the coating due to formation of protective oxide scales and microstructural changes due to in-situ heat treatment effect.

Most published papers focused on the electroless nickel-boron plating on AZ91 Mg alloy with little work on AZ31 Mg alloy. The present paper investigates the electroless nickel-boron plating AZ31 Mg alloy.

Experimental

The experimental work was preceded as follows:

- The surface of the substrates was successively ground using SiC emery paper up to 1200 mesh grit. Samples were rinsed in distilled water, supersonic degreasing in acetone and finally dried in air.
- Substrates were immersed in alkaline media (a mixture of 50 g/l NaOH and 10 g/l Na_3PO_4) for 10 min so that dust, grease etc. were removed from the surface of magnesium.
- Samples were pre activated by immersion in H_3PO_4 for 1 min followed by immersion in HFfor8 min to remove residual oxides and applying a thin layer of MgF_2.
- The substrates were mounted in this deposition bath and kept at fixed temperature for reasonable time. The bath composition and operation conditions are shown in Table (1).

Table (1): Bath Composition and Deposition Conditions

Bath composition	Concentration , g/l
Sodium borohydride ($NaBH_4$) Nickel chloride ($NiCl_2$) Ethylenediamine Sodium hydroxide Lead nitrate or Stannous Chloride	6-12 10 90 90 0.0145
Conditions: Temperature= 65-95 ºC; Deposition time=1-4 h	

Different parameters affecting the deposition of Ni-B and Ni-B-W composite coating on AZ31 Mg alloy were investigated. These parameters include concentration of sodium borohydride ($NaBH_4$), temperature, deposition time and concentration of sodium tungstate (Na_2WO_4). Based on the weight gain of the coating and the total area of the AZ31Mg alloy samples, the thickness of the formed coatings were calculated using the following equation:

$$T= W/ D*A$$

Where T is the thickness of the coating, W is the weight gain after coating, D is the density of Ni (8.91 g/cm^3) and A is the area of the coated specimens. Coated samples were investigated under the Field emission scanning electron microscope (FE-SEM).

EIS technique was used to evaluate the electrochemical behavior of the uncoated and coated samples in 0.1 M NaCl solution. Tests were done on AZ31 Mg alloy samples of 0.785 cm^2 exposed surface areas using computerized potentiostat (Autolab PGSTAT 30). A saturated calomel electrode (SCE) was used as the reference electrode and a platinum sheet as the counter electrode. The experiments were performed at room temperature over the frequency range between 1 Hz and 65 kHz at open circuit potential. The amplitude of the sinusoidal voltage signal was 10 mV.

3. Results and Discussion

3.1. Pickling and activation

Pickling is particularly critical before plating to create a uniform and catalytically active surface[15].Pickling was performed in phosphoric acid solution (400 ml/L) for 60 sec at 25ºC. The weight loss of Mg alloy reaches a maximum of 0.43 mg·cm^{-2}s^{-1} at this concentration. The increase in weight loss is attributed to the increasing in the number of hydrogen ions (decreased pH) when H_3PO_4 concentration was lower than400 mL/L. However, further increase in H_3PO_4 concentration will result in a higher concentration of PO_3^{-4}, leading to a higher tendency to produce insoluble films (mainly $Mg_3(PO_4)_2$ and $AlPO_4$) on the substrate surface slowing down the rate of Mg alloy oxidization and dissolution, leading to a decrease in weight loss.

Figure 1 shows schematic drawing of the corrosion mechanism of AZ31 Mg alloy in the etching solution. The probable reactions are shown below [16]:

$$Mg \longrightarrow Mg^{2+} + 2e^- \quad [1]$$

$$Al \longrightarrow Al^{3+} + 3e^- \quad [2]$$

$$2H^+ + 2e^- \longrightarrow H_2 \quad [3]$$

Meanwhile, the oxidized Mg and Al ions combined with : : PO_4^{3-}

$$3Mg^{2+} + PO_4^{3-} \longrightarrow Mg_3(PO_4)_2 \quad [4]$$

$$Al^{3+} + PO_4^{3-} \longrightarrow AlPO_4 \quad [5]$$

Upon increasingH_3PO_4 concentration up to 400 ml/L, enlarge etch pits are formed and tend to coalesce. The formation of such pits result in the detachment of some parts of substrate matrix with insoluble phosphate precipitation. Consequently, the etching protection by phosphate films weakened gradually with increasing concentration of H_3PO_4up to 400 ml/L with the

formation of a rough and rugged surface after pickling.

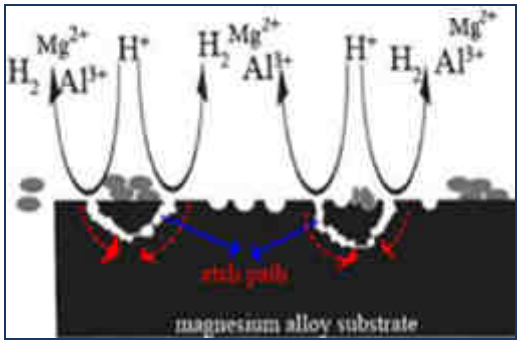

Fig.1: Schematic model for pickling of Mg alloy in 400 ml/L H3PO4

After pickling and activation in H_3PO_4 and HF solutions, respectively, coarse surfaces were obtained. This microstructure (Figure 2) on the substrate surface provides more chemical active sites for the electroless Ni-B plating and provides also surface pits for mechanically interlocking resulting in improving coating adhesion[20-21].The pickled surface must have some chemical activity for Ni ions where metallic Mg could be exposed in some areas and react with Ni ions in the electroless plating bath.

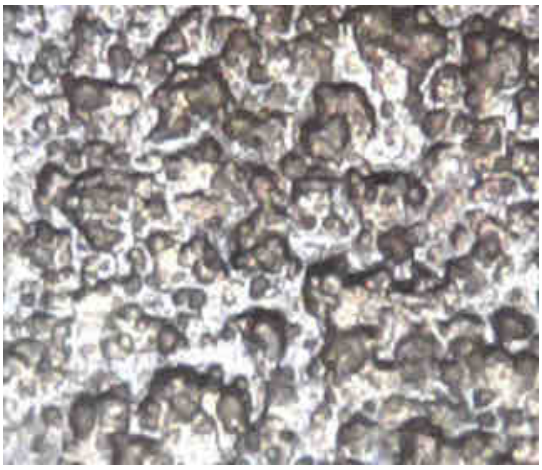

Figure 2: Optical microscopic photograph of Mg alloy after pickling in H_3PO_4 solution **(X=500)**

3.2. Electroless Ni-B coating

Electroless plating of AZ31 Mg alloy was performed in the plating bath mentioned in Table (1). The effect of different parameters including: the concentration of sodium borohydride, plating time, and plating temperature on the thickness of the formed coating were investigated. Results are presented in Tables 2-4 and Figures 3-5. Results show that the optimum concentration of $NaBH_4$ that gives the highest thickness is 8 g/l. The optimum temperature for deposition was 85^oC. The optimum time for deposition was 1 h after which the formed coating is damaged.

Scanning electron microscopic investigation (SEM) was performed on some of the coated samples (Figure 6). SEM images show the formation of compact coating layer without surface cracks. The AZ31 surface is completely covered by a densely and uniform layer; the coating bonds tightly to the substrate exhibiting good adhesion to the substrate. Figure 7 represents the cross section of the Ni-B coating formed in the presence of 8 g/L $NaBH_4$. The average coating thickness is 4.85 µm.

Table (2): Effect of concentration of $NaBH_4$ on the thickness of formed coating

$NaBH_4$ g L^{-1}	Wt gain g	Area cm^2	Thickness µm
6	0.016	3.42	5.25
8	0.026	3.20	9.10
10	0.025	3.70	7.60
12	0.018	3.42	5.90
85°C and 1 h			

Table (3): Effect of temperature on the thickness offormed coating

T/°	Wt gain g	Area cm^2	Thickness µm
65	0.006	3.71	1.80
75	0.023	3.52	7.30
85	0.030	3.52	

Table (4): Effect of deposition time on the thickness of formed coating

Time/h	Wt gain g	Area cm^2	Thickness µm
1	0.031	3.80	9.2
2	0.018	3.04	6.6
3	0.011	3.71	3.3
4	0.010	3.70	3.0
8 g/L $NaBH_4$, 85°C and 1 h			

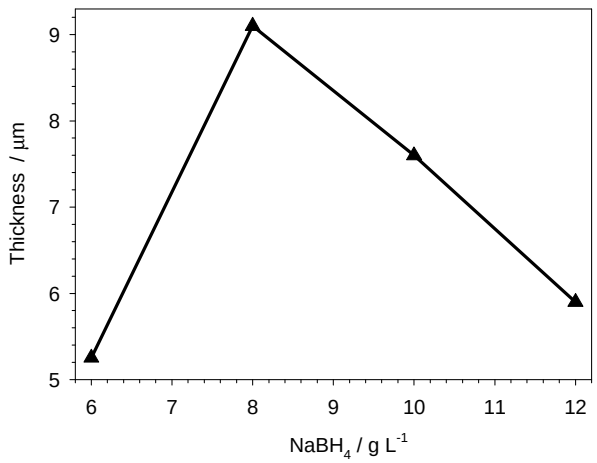

Figure 3: Effect of concentration of $NaBH_4$ (g/L) on the thickness of formed coating

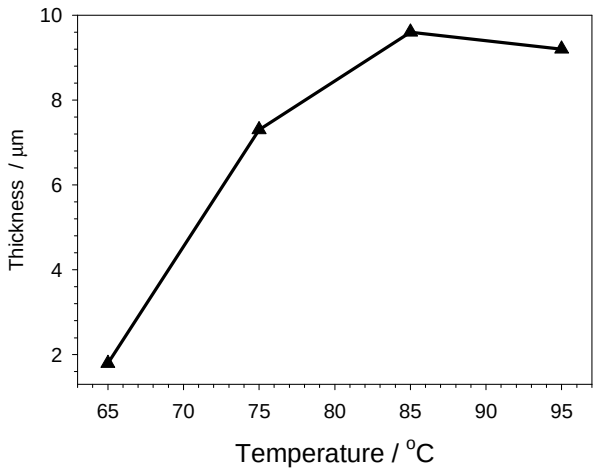

Figure 4: Effect of temperature on the thickness of formed coating

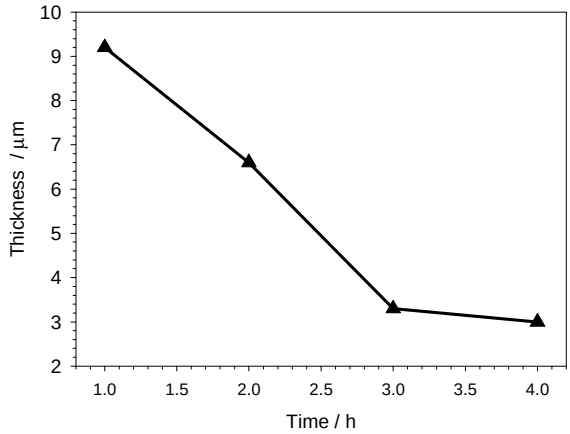

Figure 5: Effect of deposition time on the thickness of formed coating at 85°C and 1 h

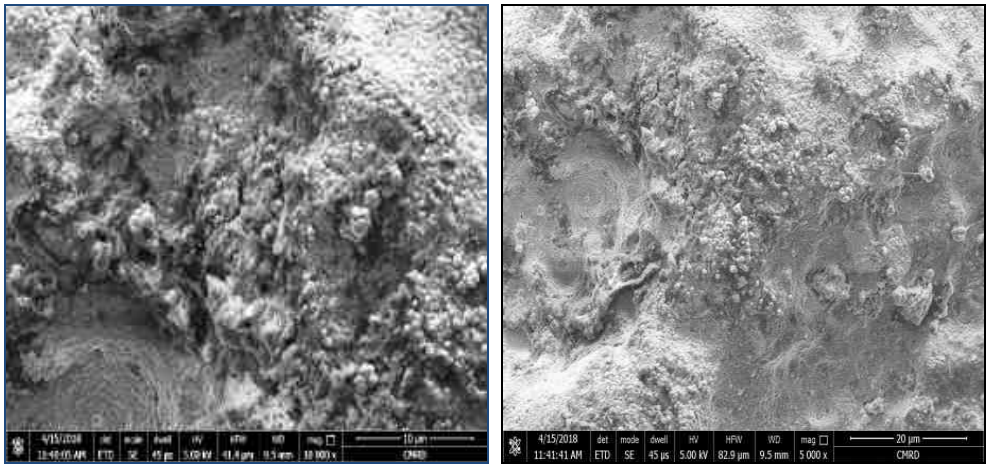

Figure 6: SEM images of Ni-B electroless coating on AZ31 Mg alloy in the presence of 8 g/L $NaBH_4$ at 85°C and 1 h

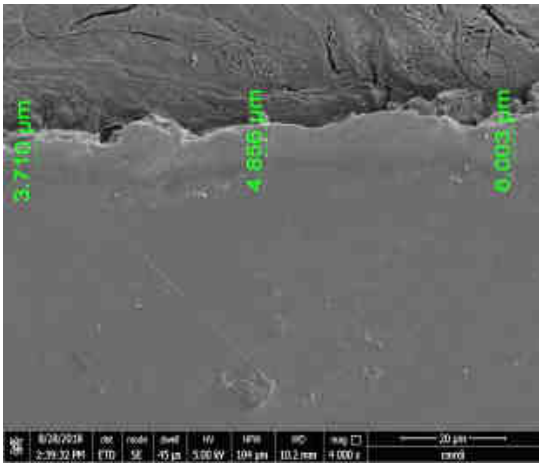

Figure 7: Cross section of Ni-B electroless coating on AZ31 Mg alloy in the presence of 8 g/L $NaBH_4$ at 85°C and 1 h

EDS measurements (Figure8) were performed on the coated AZ31 specimen. EDS spectra show peaks of Ni, Mg and O, however, no boron was detected. The nickel content of the EDS analyzed area reaches as high as 65 wt%. The absence of boron signal could be attributed to the low atomic mass of B and its low content in the coated layer. However; considering the evidenced boron signals in AES profile and element mapping performed in a previous work [15], the electroless nickel plating layer should contain B. The presence of magnesium and oxygen signals indicates the presence of magnesium oxides/hydroxides which could be attributed to the incomplete coverage of the AZ31 substrate with the Ni coating layer or to the very low thickness of the coating layer which allows the electron beam to penetrate the coat to the underneath substrate.

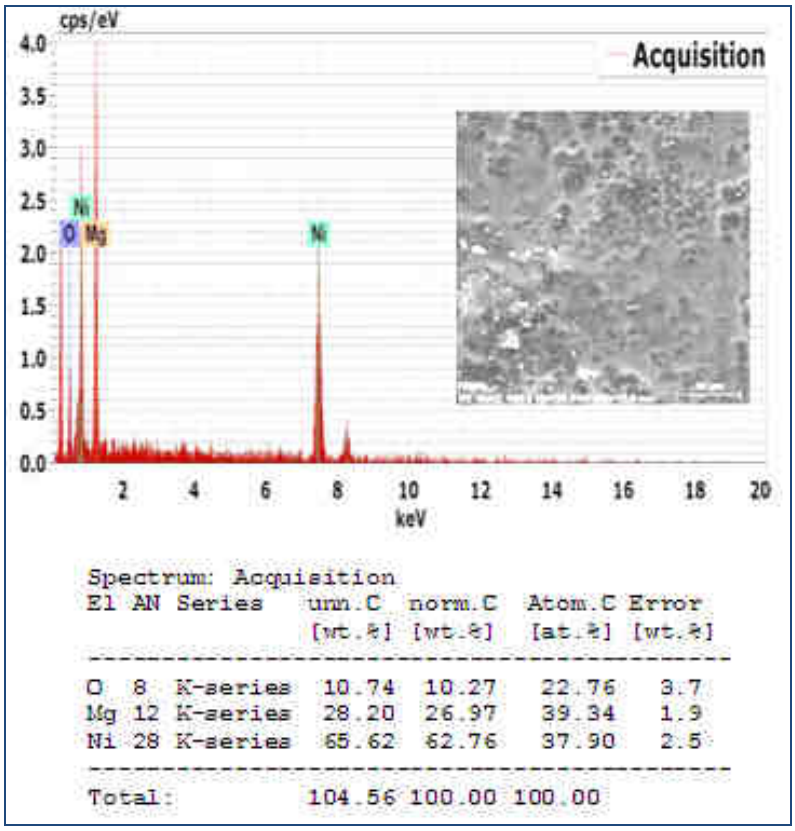

Spectrum: Acquisition

El	AN	Series	unn.C [wt.%]	norm.C [wt.%]	Atom.C [at.%]	Error [wt.%]
O	8	K-series	10.74	10.27	22.76	3.7
Mg	12	K-series	28.20	26.97	39.34	1.9
Ni	28	K-series	65.62	62.76	37.90	2.5
Total:			104.56	100.00	100.00	

Figure 8: EDS of the electroless Ni-B coating in the presence Of8 g/L $NaBH_4$ at 85^{o}C for 1 h

It is postulated that the electroless plating is a multi-steps process. Different reactions may be occurred on the pickled surface in the initial stage and on the plated surface in the later stage [17-27]. Pickling treatment results in the formation of a porous film of Mg corrosion product or magnesia film on the surface. After short time, large-size particles agglomerate to give clusters, and small homogeneous particles form in pores of the clusters. After prolonged plating, more recessed pores or intervals are gradually overlaid by a film. The film could be a result of the agglomerated Ni–B particles deposited earlier which is very thin.

After sufficient time of plating, complete coverage of the alloy surface with the complete filling of the pore areas with particles. Outside the pores, the Ni–B film gets thicker due to the deposition ofNi–B particles. Mg and Al with few corrosion products could be only detected after the pickling treatment. During plating, Ni and O signals start to appear indicating the formation of Mg oxides or hydroxides. The appearance of Ni peak associated with the gradual disappearance of the Mg peak points to the deposition of Ni on the alloy surface. With time, nickel peaks are intensified, indicating the complete coverage of AZ31 surface with the deposited Ni. It is proposed that in the initial electroless deposition of Ni–B directly on pickled AZ31, following reactions are involved:

$$Mg + Ni^{+2} \longrightarrow Mg^{+2} + Ni \quad [6]$$

$$Mg + 2H_2O \longrightarrow Mg(OH)_2 + H_2 \quad [7]$$

$$2Al + 6H_2O \longrightarrow 2Al(OH)_2 + 3H_2 \quad [8]$$

$$MgO_{(\text{originally formed on surface})} + H_2O \longrightarrow Mg(OH)_2 \quad [9]$$

After pickling the substrate is partially covered by a porous magnesia film. On such a surface, plating may proceed in two different ways. The first approach involves the grown of Ni nuclei on the magnesia film covered areas around the pores as the favored place for nucleation. The second approach involves the nucleation of Ni plating through reaction (6) which occurs preferentially around the edges of magnesia film pores in the substrate surface. Reactions (7) and (8) are easier to occur in the central area of a film pore, where is more accessible to water. The hydrogen evolved due to from reactions (7) and (9) keeps stirring central pore area making Ni nuclei deposition difficult. The deposited Ni spreads from the pore edges till the complete coverage of the pores. On the other hand, the presence of metallic Mg lead to the rapid formation of nickel nuclei (reaction (6)), resulting in the formation of homogeneous Ni particles in the exposed substrate areas. Reactions (7) and (8) occurring mainly in the film pore central areas can lead to surface alkalization. An increase in pH value is beneficial to B deposition. The following reactions maybe involved in electroless nickel–boron plating as well:

$$BH_4^- + 4\,Ni^{2+} + 8\,OH^- \longrightarrow 4Ni + BO_2^- + 6H_2O \quad [10]$$

$$2\,BH_4^- + 2H_2O \longrightarrow 2B + 2OH^- + 5H_2 \quad [11]$$

These two Ni and B deposition reactions can be speeded up at a higher pH. When the dissolution of the substrate is considerable, a large amount of B will be incorporated in the Ni plating in the initial plating stage. The deposition of fresh nickel particles in the initial plating stage has a catalytic effect on plating enabling continuous reduction reactions of Ni and Ni–B on the surface. Simultaneously, the deposited Ni and Ni–B particles can join together and finally spread out to the whole surface of the substrate. After deposition of a relatively thick layer of Ni/Ni–B coating on the alloy surface, the dissolution of the substrate is ceased and the surface alkalization effect gets weaker. Ni reduction reaction (11) will dominate the plating process o the slowdown of reactions (10) and (8). Consequently, the B content becomes lower in the plating layer.

The electroless plating process can be summarized as follows: in the initial deposition stage, the substrate surface possesses a large number of active sites for rapid Ni replacement of Mg and nucleation reactions, forming small nickel nuclei from edge to center in the surface film pores. Boron atoms may also be adsorbed to the Ni surface, and promote the formation of new nuclei. Meanwhile, the corrosion of the substrate results in the deposition of Ni_2B. After the substrate surface is completely covered by Ni/Ni–B, the freshly deposited nodular nickel acts as a catalyst for continuous Ni deposition reaction and the main electroless plating process becomes from Ni replacement to Ni deposition. Together with slow deposition ofNi_2B, deposited nickel particles are built up layer by layer to form a smooth and dense Ni–B coating.

3.3. Electrochemical corrosion performance

Enhancement of corrosion resistance is an important goal of electroless Ni-B plating on a Mg alloy. EIS experiments were performed to investigate the corrosion resistance of the deposited electroless plated Ni-B on the tested AZ31 Mg alloy. Figure 9 shows Nyquist plots of the uncoated alloy as well as the Ni–B coating in 3.5 wt.% aqueous NaCl solution at the free corrosion potential (E_{corr}). EIS spectra show basically one-semicircle in the measuring frequency region. The observed semicircles differ in diameters which denote a simple and similar corrosion process with different corrosion rates [28-29]. The one-semicircle capacitive spectrum indicates the formation a good quality coating [30]. A simple equivalent circuit can be used to simulate the EIS behavior as seen in Figure10, where R_s is a solution resistance, CPE represents a constant phase element corresponding to the capacitance of the electrode surface, and R_p is a polarization resistance. It is shown that the Ni–B coating has much higher polarization resistance than the bare AZ91D substrate. The polarization resistance reaches as high as 21000 ohm compared to only 460 ohm obtained for the uncoated alloy indicating a large enhancement of the corrosion resistance of the alloy.

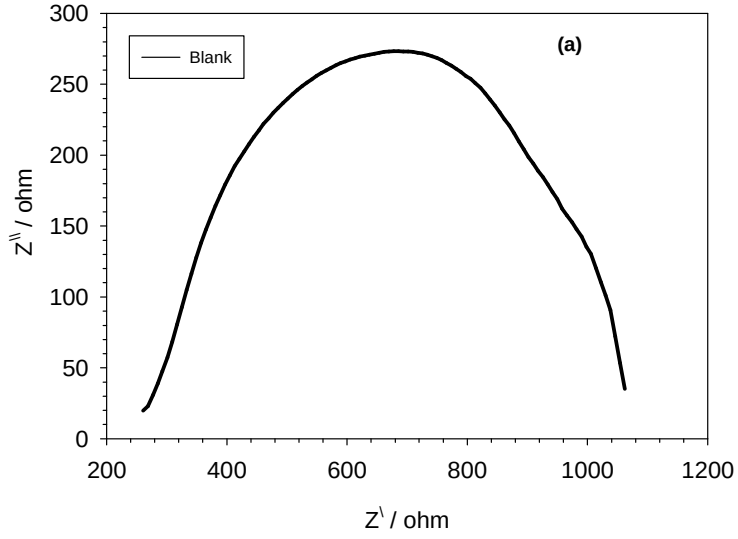

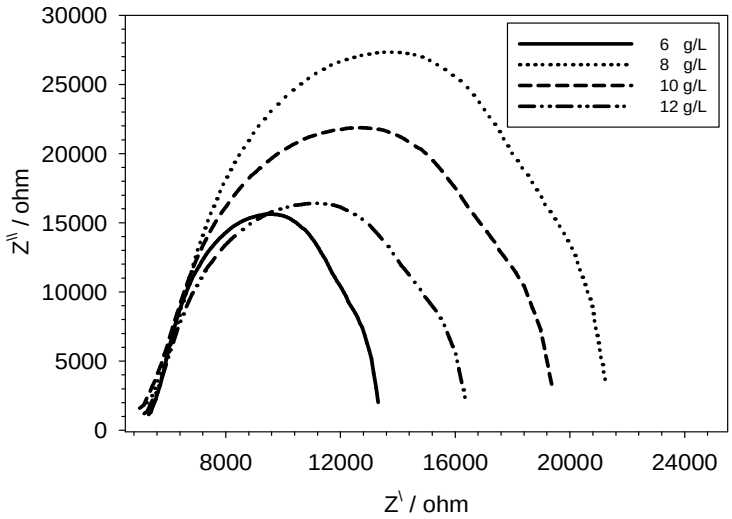

Figure 9: EIS spectra of uncoated (a) and electroless Ni-$B_{(6\text{-}12\ g/L)}$ coated (b) AZ31 Mg alloying 3.5 wt.%NaCl solution.

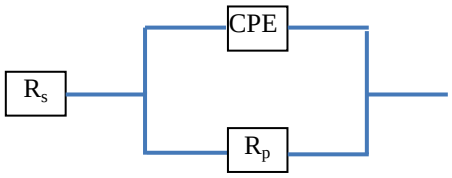

Figure 10: The equivalent circuit for curve-fitting of the EIS results

4. Conclusions

1. Electroless Ni-B-W coating was performed on the AZ31 alloy in the path mentioned in Table (1). Pickling was performed in phosphoric acid solution (400 ml/L) for 60 sec at 25°C while activation was performed in HF (40%) for 8 min. The highest thickness of the Ni-B coating was obtained in the presence of 8 g/L $NaBH_4$at 85°C and 1 h.
2. The electroless nickel coating exhibits a uniform surface with an average thickness of 4.85 µm. The EDS analysis shows peaks of Ni, Mg and O but not B. The absence of B signal was attributed to its light weight and low content in the coat.
3. EIS measurements indicates the high improvement of the the corrosion resistance of AZ31 magnesium alloy after the electroless Ni–B plating.
4. Electroless plating mechanism suggests rapid Ni replacement of Mg as Ni nucleation reaction starts at active sites in the metallic areas along the edges of magnesia film pores on the pickled AZ31 surface at the initial plating stage. The dissolution of the substrate leads to surface alkalization, resulting in the deposition of Ni–B. In the later stage, electroless deposition of Ni dominates the plating process.

5. References:

1. M.K. Kulekci, Magnesium and its alloys applications in automotive industry, Int J Adv Manuf Technol, 39 (2008)851–865.
2. C. Ying-liang, Q. Ting-wei, W. Hui-min, Z. Zhao, Comparison of corrosion behaviors of AZ31, AZ91,AM60 and ZK60 magnesium alloys, Transactions of nonferrous metals society of china, 19(2009)517-524.
3. R.K. Singh Raman, R.K.,''The Role of Microstructure in Localized Corrosion of Magnesium Alloys'', Metallurgical and Materials Transactions A, 35A (2004) 2525-2531.
4. S. Housh and B Mikucki, Selection and Application of Magnesium and Magnesium Alloys, Properties and Selection: Non Ferrous Alloys and Special Purpose Materials, Vol 2, ASM Hand Book, ASM International, 1990, p 455-479.
5. Z. Shao, Z. Cai, R. Hu, S. Wei, The study of electroless nickel plating directly on magnesium alloy, Surf. Coat. Technol., 249 (2014) 42-47.

6. E. Correa, A.A. Zuleta, M. Sepúlveda, L. Guerra, J.G. Castaño, F. Echeverría, H. Liu, P. Skeldon, G.E. Thompson, Nickel–boron plating on magnesium and AZ91D alloy by a chromium-free electroless process, Surf Coat Technol, 206 (2012) 3088-3093.
7. G.L. Song, Corrosion Prevention of Magnesium Alloys, A volume in Wood head Publishing Series in Metals and Surface Engineering, (2013), 370–392.
8. F. Bülbül, Ni-B Coating Production on Magnesium Alloy by Electroless Deposition, IJMMI, 9 (2015) 772-775.
9. Z.C. Wang, F. Jia, L. Yu, Z.B. Qi, Y. Tang, G.L. Song, Direct electroless nickel–boron plating on AZ91D magnesium alloy, Surf. Coat. Technol., 206 (2012) 3676–3685.
10. E. Correa, A. A. Zuleta, L. Guerra, G. E. Thompson, Coating development during electroless Ni–B plating on magnesium and AZ91D alloy, Surf. Coat. Technol.,232 (2013)784-794.
11. L. Bonin, N. Bains, V. Vitry, A.J. Cobley, Electroless deposition of nickel-boron coatings using low frequency ultrasonic agitation: Effect of ultrasonic frequency on the coatings,Ultrasonics,77(2017) 61-68.
12. J. Zhang, Z.H. Xie, H. Chen, C. Hu, L. Li, B. Hu, Z. Song, D. Yan, G. Yu, Electroless deposition and characterization of a double-layered Ni-B/Ni-P coating on AZ91D Mg alloy from eco-friendly fluoride-free baths, Surf. Coat. Technol., 342 (2018) 178-189.
13. E. Correa, A.A. Zuleta, L. Guerra, M.A. Gómez, J.G. Castaño, F. Echeverría, H. Liu, P. Skeldon, G.E. Thompson, Tribological behavior of electroless Ni–B coatings on magnesium and AZ91D alloy, Wear, 305 (2013) 115-123.
14. A. Mukhopadhyay, T. K. Barman, P. Sahoo, Wear and friction characteristics of electroless Ni-B-W coatings at different operating temperatures, Mater. Res. Express.,5,2018.
15. Z.C. Wang, F. Jia , L. Yu, Z.B. Qi, Y. Tang, G.-L. Song, Direct electroless nickel–boron plating on AZ91D magnesium alloy, Surf Coat Techn, 206 (2012) 3676–3685.
16. ZHX. F. Chen, SR X., JL Zhou, ZW Song, G. Yu, Studies of Several Pickling and Activation Processes for Electroless Ni-P Plating on AZ31 Magnesium Alloy, Journal of The Electrochemical Society, 162 (3) D115-D123 (2015)
17. Y. P. Zhu, G. Yu, B. N. Hu, X. P. Lei, H. B. Yi, and J. Zhang. Electrochemical behaviors of the magnesium alloy substrates in various pretreatment solutions, Appl Surf Sci, 256 (2010) 2988.
18. U. C. Nwaogu, C. Blawert, N. Scharnagl, W. Dietzel, and K. U. Kainer, Influence of inorganic acid pickling on the corrosion resistance of magnesium alloy AZ31 sheet, Corros. Sci., 51 (2009) 2544.
19. X. P. Lei, G. Yu, X. L. Gao, L. Y. Ye, J. Zhang, and B. N. Hu, A study of chromium–free pickling process before electroless Ni–P plating on magnesium alloys, Surf Coat Technol. 205 (2011) 4058.
20. J E Gray, B Luan. Protective coatings on magnesium and its alloys–a critical review, J. Alloys Compd. 336, 88 (2002).
21. C. Gu, J. Lian, G. Li, L. Niu, and Z. Jiang, Electroless Ni–P plating on AZ91D magnesium alloy from a sulfate solution, J. Alloys Compd. 391, 104 (2005).
22. G.O. Mallory, B. Hajdu, “Troubleshooting Electroless Níckel Plating Solutions”, Ed. AESF, New York, 1990, p. 238.
23. Q.L. Rao, B. Gang, Q.H. Lu, H.W. Wang, X. Fan, Microstructure evolution of electroless Ni-B film during its depositing process, Appl. Surf. Sci. 240 (2005) 28.
24. R. Well, "Characterization of deposits, coatings and electroforms, Part 4, mechanical properties elastic behavior and yielding, "Plating and surface finishing, 85(3) (1998) 38-39.
25. M Zhang, X. Wang, X. Yang, J. Zou, S Liang, "Arc erosion behaviors of $AgSnO_2$ contact materials prepared with different SnO_2 particle sizes", Trans. Nonferrous Met. Soc. China 26(2016) 783−790.
26. Y.L. Lo, B.J. Hwang, Decomposition of sodium borohydride in an electroless nickel bath, Ind. Eng. Chem. Res. 33 (1994) 56.
27. M.F. He, L. Liu, Y.T. Wu, Z.X. Tang, W.B. Hu, Improvement of the properties of surface-modified AZ91D magnesium alloy, Corros.Sci.50 (2008) 3267.
28. G. Galicia, N. Pébére, B. Tribollet, V. Vivier, Local and global electrochemical impedances applied to the corrosion behavior of an AZ91 magnesium alloy, Corros Sci, 51 (2009) 1789.
29. M. Anik, G. Celikten, Analysis of the electrochemical reaction behavior of alloy AZ91 by EIS technique in H_3PO_4/KOH buffered K_2SO_4 solutions, Corros. Sci., 49 (2007) 1878.
30. H. Ardelean, I. Frateur, P. Marcus, Corrosion mechanisms in theory and practice, Corros. Sci. 50 (2008) 1907.